

Self-Assembled Monolayers of Alkanethioacetates on Au(111) in Ammonium Hydroxide Solution

Taesung Park,[†] Hungu Kang,[†] Eisuke Ito,[‡] and Jaegeun Noh^{†,§,¶,*}

[†]Department of Chemistry, Hanyang University, Seongdong-gu, Seoul 04763, Korea

[‡]Chemical Materials Evaluation and Research Base (CEREBA), Higashi 1-1-1, AIST Central 5-2, Tsukuba, Ibaraki 305-8565, Japan

[§]Institute of Nano Science and Technology, Hanyang University, Seongdong-gu, Seoul 04763, Korea

[¶]Research Institute for Convergence of Basic Science, Hanyang University, Seongdong-gu, Seoul 04763, Korea. *E-mail: jgnoh@hanyang.ac.kr

Received November 6, 2020, Accepted December 11, 2020, Published online December 21, 2020

To shed light on the effects of NH₄OH deprotection reagent on the formation of self-assembled monolayers (SAMs) from alkanethioacetates on Au(111), we examined the surface structure and adsorption conditions of SAMs on Au(111) prepared in a 1 mM octanethioacetate (C8SAc) methanol solution and in a 1 mM methanol solution formed after *in situ* deprotection of C8SAc by NH₄OH. Scanning tunneling microscopy (STM) imaging revealed that direct adsorption of C8SAc on Au(111) created only disordered SAMs regardless of the polarity of solvent (methanol, DMF, and hexane). In contrast, highly ordered SAMs with a well-ordered c(4 × 2) phase were formed via *in situ* deprotection of C8SAc by NH₄OH (deprotection condition: 30.7 mM NH₄OH, 323 K, and 3 h). X-ray photoelectron spectroscopy measurements also showed that the SAMs formed via *in situ* deprotection show uniform adsorption, whereas those prepared by direct adsorption show very complicated adsorption, which agrees well with STM results.

Keywords: Self-assembled monolayers, Alkanethioacetate, Adsorption, Scanning tunneling microscopy, X-ray photoelectron spectroscopy

Introduction

The surface and interface properties of metal or semiconductor substrates are readily tunable by the formation of self-assembled monolayers (SAMs) via adsorption of various adsorbates with different docking groups and molecular backbones.^{1–26} Therefore, SAMs have been widely utilized in many technological applications such as sensors, bio-interfaces, electronic devices, and surface nanopatterning.^{1–6} Alkanethiols are the compound most commonly used on gold for SAM preparation because at saturation coverage they can form a nicely ordered monolayer with the ($\sqrt{3} \times \sqrt{3}$)R30° or c(4 × 2) packing structure.^{1,2,19,24,25} However, one drawback to using thiols is that in solution they can readily transform by oxidation to disulfides or sulfonate during SAM formation.^{8,27–29} To minimize this undesirable side reaction, other precursors such as chemically stable thiocyanates^{30–35} or acetyl-protected thiols (thioacetate)^{26,27,29,36–50} have been developed for SAM preparation. Various acetyl-protected thiols in particular have often been used for the preparation of SAM-based electronic devices via *in situ* deprotection of acetyl groups.^{36–40} The charge transport properties of SAM-based devices are significantly influenced by the degree of structural order and adsorption geometry of SAMs.^{38,51} Therefore, structural control over SAMs is

critical for their practical use and so that SAM surface structures should also be understood.

Direct adsorption of thioacetate on gold surfaces in solution results in the formation of loosely packed and poorly ordered SAMs compared to their thiol analogs.^{29,41,42,46,48} Scanning tunneling microscopy (STM) observations showed that SAMs derived from alkanethioacetates^{45,48} or aromatic thioacetate^{43,44} on Au(111) deployed in predominantly disordered phase. Spectroscopic measurements also showed that surface coverage of alkanethioacetate SAMs is lower than that of thiol SAMs with identical alkyl chains.²⁹ Moreover, ellipsometric measurements demonstrated that the adsorption kinetics of aromatic thioacetate or alkanethioacetate on gold surfaces is slower than that of their thiol analogs.⁴² Due to the inferior structural quality of organic thioacetate SAMs on gold, *in situ* deprotection of acetyl-protecting groups is required for enhancing the structural quality of SAMs. This deprotection step in solution is involved in structural conversion of a thioacetate to a free thiol. For this purpose, acid- or base-catalyzed deprotection reagents such as HCl,⁴⁸ H₂SO₄,³⁹ NH₄OH,^{26,27,36,41,48–50} N(CH₂CH₃)₃,^{38,47,50} *n*-CH₃CH₂CH₂NH₂,⁴⁸ NaOH,⁵² and KOH⁴⁸ have been used and the formation and structural characteristics of the resulting organic thioacetate SAMs on metals have been extensively characterized. Tetrabutylammonium cyanide

has also been used as a deprotection reagent.^{8,28,46} It has been reported that acetyl-protected aromatic dithiol, after deprotection by NH_4OH on Au(111), would form multi-layer films, whereas closely packed monolayers with a higher structural order would form after deprotection by triethylamine.⁵⁰ Near-edge X-ray absorption fine structure spectroscopy measurements revealed that SAM derived from acetyl-protected terphenylthiol on GaAs had more upright orientation using a low concentration of NH_4OH solution (1 mM) compared to a high concentration solution (160 mM), implying that concentration of NH_4OH affects significantly the final structure of thioacetate SAMs.²⁶ On the other hand, STM observations revealed that SAMs on Au(111) formed after *in situ* deprotection of decanethioacetates by NH_4OH had predominantly disordered phase, but some ordered domains also existed.⁴⁸ Although NH_4OH is the most frequently used deprotecting reagent for the preparation of thioacetate SAMs, few molecular-scale STM reports exist describing how much NH_4OH deprotection reagent affects the surface structure and ordering of thioacetate SAMs on Au(111).

To shed light on this issue, we used STM and X-ray photoelectron spectroscopy (XPS) to examine and compare the surface structure and adsorption state of SAMs on Au(111) prepared by direct adsorption of octanethioacetate [$\text{CH}_3(\text{CH}_2)_7\text{SCOCH}_3$, C8SAc] and via *in situ* deprotection of C8SAc by NH_4OH . Herein we report the first STM results showing that C8SAc molecules could form well-ordered SAMs on Au(111) with a $c(4 \times 2)$ packing structure via sufficient deprotection by NH_4OH .

Experimental Section

C8SAc was synthesized by refluxing a mixture of 1-bromooctane and potassium thioacetate in ethanol at room temperature (RT) for 3 h, according to the reported method.⁴⁶ Single crystal Au(111) substrates for SAM preparation were obtained by the vacuum deposition of gold onto mica, as addressed in the literature.⁷

To examine the effects of NH_4OH deprotection reagent on the formation of C8SAc SAMs on gold surfaces, we prepared two kinds of SAM samples on Au(111) prepared by direct adsorption of C8SAc in a pure solvent and by adsorption of C8SAc in solution containing a deprotection reagent of NH_4OH at room temperature (RT) for 24 h (Figure 1). Solvent effects on SAM formation of C8SAc in a pure solvent were also examined using three kinds of solvents: methanol (polar protic solvent, dipole moment: 1.78 D), *N,N'*-dimethylformamide (DMF, polar aprotic solvent, dipole moment: 3.86 D), and n-hexane (nonpolar solvent). *In situ* deprotection of acetyl group in C8SAc was made by adding 10 μL of NH_4OH (aqueous 30%) solution in a 2.5-mL vial containing a 1 mM C8SAc methanol solution and then this mixed solution was incubated at 323 K for 3 h. Concentration of NH_4OH in this mixed solution is 30.7 mM. For SAM formation, the Au(111) substrates were

immersed in the mixed solution after cooling to RT for 24 h. The prepared SAM samples were rinsed with methanol and dried in a stream of N_2 gas before surface characterization.

STM measurements were conducted with a NanoScope E (Veeco, Santa Barbara, CA) in an ambient condition. STM images were obtained using bias voltages between 400 and 600 mV and tunneling currents between 300 and 650 pA. A Theta Probe (Thermo Fisher Scientific Inc., U.K.) with an Al $K\alpha$ X-ray source (1486.6 eV) was used for XPS measurements. The binding energy was calibrated with the Au $4f_{7/2}$ peak at 84.0 eV. XPS spectra were obtained using a curve-fitting analysis.

Results and Discussion

It has been reported that solvent properties are an important factor for determining the structural order and packing density of organic thiolate SAMs on Au(111).^{1,44,53–56} STM observations elucidated that alkanethiol SAMs on Au(111) prepared in ethanol and DMF have a high structural quality with densely packed and largely ordered domains, whereas those prepared in hexane (heptane) and toluene have less ordered SAMs.^{53–56} This result means that the structural quality of alkanethiol SAMs could be improved by using a solvent with higher polarity compared to a nonpolar solvent. It is reasonable to consider that relatively strong hydrophobic interactions between nonpolar alkyl chains in alkanethiol SAMs and nonpolar solvents such as alkanes effectively prevent the formation of an ordered crystalline phase.⁵⁶ On the other hand, the surface morphology of amine-terminated thiolate SAMs was significantly modified by polar protic solvents compared to polar aprotic or nonpolar solvents, which results from strong hydrogen bond interactions between terminal amine groups of SAMs and polar protic solvent molecules.⁵⁷

To understand solvent effects on SAM formation of C8SAc on Au(111), we used three different solvents: methanol, DMF, and hexane. Figure 2 exhibits STM images showing the surface morphology of SAMs of C8SAc on Au(111) prepared in methanol, DMF, hexane at 298 K for 24 h. Direct adsorption of C8SAc on Au(111) caused mainly disordered SAMs composed of many bright aggregates regardless of the polarity of solvent used, as shown in Figure 2. Vacancy islands (dark regions) that are a good proof for the formation of chemisorbed monolayers^{1,2} were clearly observed when methanol and DMF solvents were used for SAM formation (Figure 2(a) and (b)), though not with hexane solvent (Figure 2(c)), implying that polar solvents could facilitate the formation of SAMs from organic thioacetates compared to nonpolar solvents. For this reason, it is suggested that the oxygen atoms in methanol and DMF can attack the acetyl carbon of thioacetate as a nucleophile in the process of surface-mediated deacetylation, often referred to as the general base catalysis mechanism.⁵⁸ The resulting acetate leaving group can subsequently be

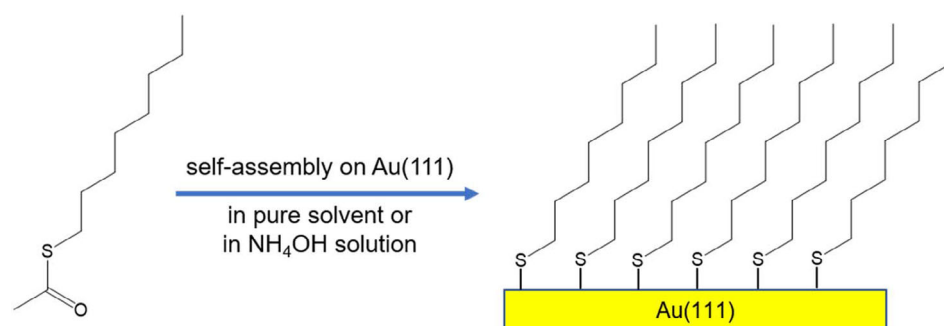


Figure 1. A schematic illustration describing the formation of SAMs on Au(111) by adsorption of C8SAc in pure solvent or NH₄OH solution.

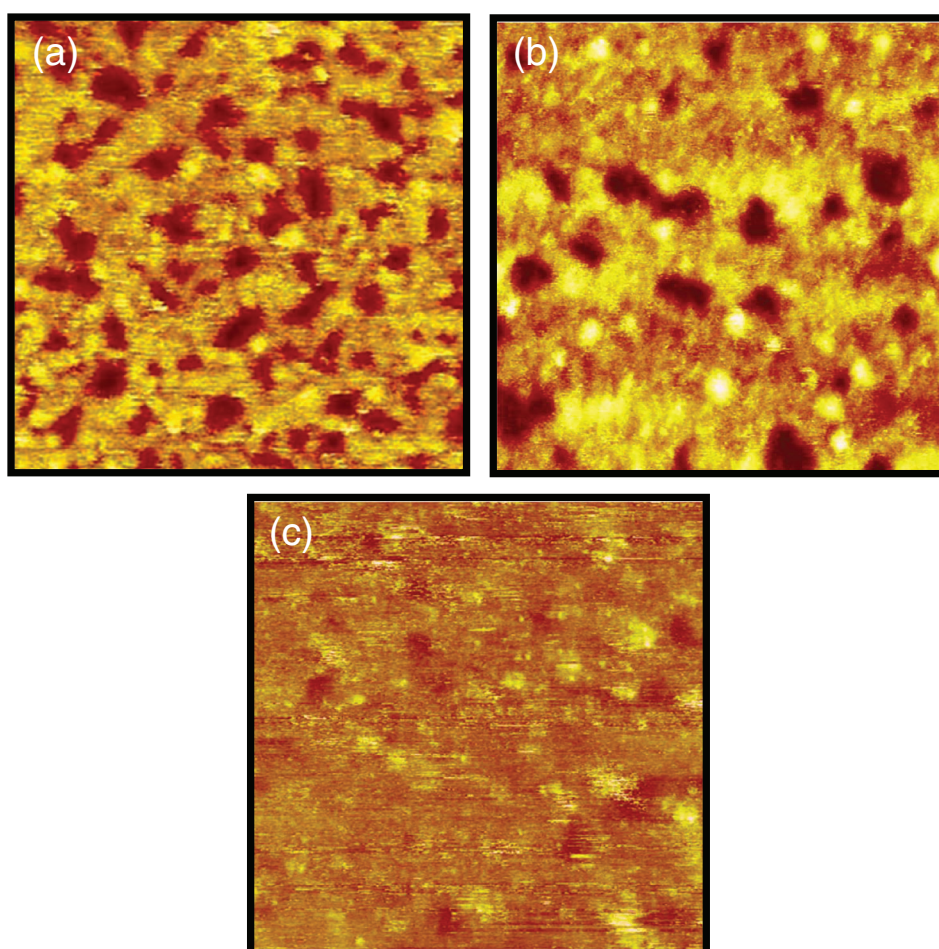


Figure 2. STM images showing the surface morphology of SAMs on Au(111) by direct adsorption of C8SAc in pure solvents: (a) methanol (b) DMF, and (c) hexane at RT for 24 h. Scan sizes of all STM images are $60 \times 60 \text{ nm}^2$.

efficiently removed from the surface in the polar solvent. However, we found that solvent is not a very critical factor for improving the structural order of SAMs of alkanethioacetates on Au(111). Our results obtained herein are in good agreement with previous reports showing that SAMs prepared by direct adsorption of organic thioacetate on gold surfaces had an inferior structural quality with lower surface coverage and less ordered phase compared to their thiol analogs.^{29,41,42,46,48}

These intrinsic structural characteristics for thioacetate SAMs can be attributed to both the lower adsorption ability of sulfur because of the binding of electron withdrawing acetyl group and the steric hindrance of acetyl group during adsorption of sulfur in thioacetates, demonstrated by previous kinetic study.⁴² Organic thiocyanates (RS-CN) have shown similar adsorption tendency showing that adsorption of thiocyanates on Au(111) is much slower than that of thiols.^{29,35}

Due to the low structural quality of SAMs on gold formed by various thioacetates, *in situ* deprotection processes of acetyl group in thioacetates have been developed. As addressed in the introduction, the various deprotection reagents are used to improve SAM structural quality. Among them, NH_4OH is the most popular for preparation of thioacetate SAMs.^{26,27,36,41,48–50} However, STM measurements by Singh *et al.* reported that monolayers on Au(111) formed via *in situ* deprotection of decanethioacetate (2.5 mM) by NH_4OH (2.5 mM) in ethanol at RT for 1 h were composed of several structural phases showing a predominantly disordered phase and small domains of a striped phase and a standing-up ($\sqrt{3} \times \sqrt{3}$)R30° phase.⁴⁸ ^1H NMR study showed that deprotection rate of decanethioacetate (58 mM) by NH_4OH (115 mM) in CD_3OD at RT is very slow (deprotection ratio of 58% even after 48 h).⁴⁸ Therefore, it is reasonable to assume that previously used deprotection conditions (NH_4OH 2.5 mM, RT, and 1 h) were not sufficient for conversion of decanethioacetate to decanethiol. As a result, less ordered SAMs were formed. Moreover, more than 70% of aromatic thioacetate (0.25 mM) in ethanol containing 30 mM NH_4OH at 328 K for 1 h can be converted to the aromatic thiol.²⁶ Based on these previous results, we carefully selected *in situ* deprotection conditions (30.7 mM NH_4OH , 323 K, and long deprotection process of 3 h) that can complete the conversion of the C8SAc (1 mM) to C8SH. After this deprotection step, the solution was cooled down to RT. Then the SAM samples were prepared by dipping clean Au(111) substrates in this solution for 24 h. STM images in Figure 3 clearly exhibit that the resulting SAMs on Au(111) have densely packed and highly ordered molecular arrangements. Ordered SAMs were fully covered with Au(111) surface (Figure 3(a)) and the ordered domains are described as a well-known $c(4 \times 2)$ superlattice (Figure 3(b)) as observed for densely packed SAMs formed by various n-alkanethiols.^{1,2,25,35,55,59–62} The observed

surface characteristics such as ordered domains and vacancy islands are identical with those of SAMs prepared by octanethiol (C8SH), as demonstrated by previous works.^{25,35,55,59–62} In this STM study, we revealed that well-ordered SAMs could be formed on Au(111) by acetyl-protected alkanethiols using a suitable *in situ* deprotection process.

To shed light on the effects of NH_4OH deprotection reagent on the formation of thioacetate monolayers, we also examined and compared via XPS the adsorption state of octanethiolate SAMs on Au(111) prepared in a 1 mM C8SAc methanol solution and in a 1 mM methanol solution formed after *in situ* deprotection of C8SAc by NH_4OH . XPS measurements showed a considerable difference in the S 2p spectra of two thiolate SAMs on Au(111) (Figure 4). This result means that the adsorption conditions of sulfurs in octanethiolate SAMs on Au(111) were markedly influenced by SAM preparation methods. It is well-known that the sulfur 2p spectra can appear as a doublet ($2p_{3/2}$ and $2p_{1/2}$ peaks) by spin-orbital splitting and with relative intensity of 2:1.^{8,31–33,55,63–66} Figure 4(a) displays three different S 2p peaks (labeled A, B, and C) for SAMs on Au(111) prepared by adsorption of C8SAc in pure methanol at RT for 24 h. Their $2p_{3/2}$ peaks were observed at 162.2 (peak A), 161.3 (peak B), and 163.8 eV (peak C). Many XPS studies for alkanethiolate SAMs on gold revealed that the A and B peaks are originated from the chemisorption of sulfurs and the C peak is due to the physisorption of sulfur.^{8,31–33,55,63–66} In general, the A peak was dominant for closely packed thiolate SAMs, whereas the B peak was observed for loosely packed SAMs and/or when atomic sulfurs existed on the surface.^{8,55,63–66} The C peak often appeared in the SAMs formed by complicated thiol derivatives or in the unrinsed SAMs.^{63,64} Therefore, the presence of three S 2p peaks in the SAMs strongly implies that the SAMs have inhomogeneous sulfur adsorption states. As a result, disordered phases could form, as

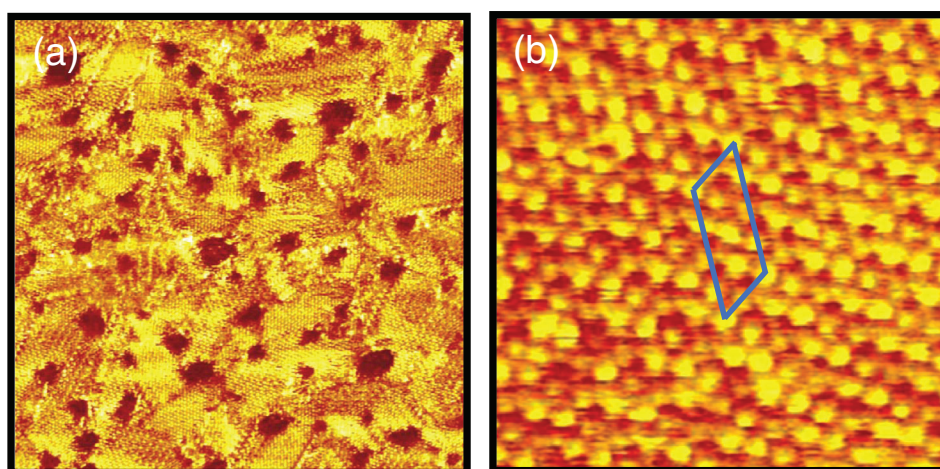


Figure 3. STM images showing the formation of well-ordered SAMs on Au(111) formed via *in situ* deprotection process of C8SAc by NH_4OH . Scan sizes are (a) $60 \times 60 \text{ nm}^2$ and (b) $8 \times 8 \text{ nm}^2$.

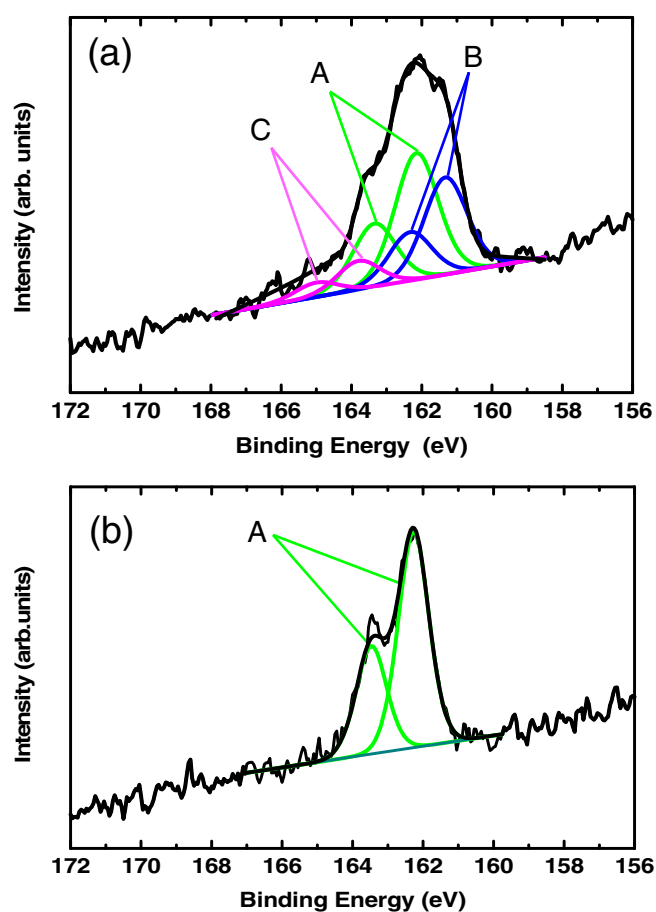


Figure 4. XPS spectra in the region of S 2p of SAMs on Au(111) formed by (a) direct adsorption of C8SAc in methanol and (b) via *in situ* deprotection of C8SAc by NH_4OH .

shown in the STM image of Figure 2(a). The relative intensity ratio of each S 2p peak (peak A, B, and C) versus Au 4f was measured to be 0.0053, 0.0041, and 0.0012, respectively. The intensity ratio of chemisorbed sulfurs (peak A + peak B) versus physisorbed sulfurs (peak C) was calculated to be 7.83, suggesting that the direct adsorption of C8SAc in methanol also generates mostly chemisorbed monolayers. In contrast, only one chemisorbed S 2p peak (peak A) was observed for the SAMs prepared via *in situ* deprotection of C8SAc by NH_4OH (Figure 4(b)), implying the formation of a uniform monolayer. High-resolution STM observations revealed that the resulting SAMs have well-ordered domains with a closely packed $c(4 \times 2)$ superlattice (Figure 3), which is consistent with XPS results. Actually, similar XPS spectra were also observed for well-ordered alkanethiol SAMs.^{64,66} The relative intensity ratio of S 2p peak (peak A) versus Au 4f was measured to be 0.0071, which is 1.34 times larger than that found for SAMs prepared by direct adsorption in methanol (0.0053). From our XPS measurements, we revealed that SAMs of C8SAc with uniform interface structure were formed using a suitable *in situ* deprotection process by NH_4OH , whereas

those formed by adsorption of C8SAc in methanol have a very complicated interface structure.

Conclusion

The structure and adsorption states of SAMs on Au(111) prepared by direct adsorption of acetyl-protected C8SAc and via *in situ* deprotection of C8SAc by NH_4OH were examined by STM and XPS to elucidate the effect of NH_4OH deprotection reagent on the formation and structural order of the SAMs. STM observations revealed that adsorption of C8SAc on Au(111) in pure solvents created mainly disordered SAMs with many bright aggregates regardless of the polarity of solvent used. In contrast, highly ordered SAMs with a closely packed $c(4 \times 2)$ phase were formed via *in situ* deprotection step at 323 K for 3 h. XPS measurements also elucidated that the SAMs formed via the suitable *in situ* deprotection process have uniform interface structure, while those prepared by direct adsorption in methanol have very complicated interface structure. In this study, we clearly showed that highly ordered thiolate SAMs on Au(111) can be prepared by acetyl-protected alkanethiols using a suitable *in situ* deprotection process.

Acknowledgments. This work was supported by the National Research Foundation of Korea (NRF) funded by the Ministry of Education (NRF-2012R1A6A1029029, NRF-2018R1D1A1B07048063, and NRF-2020R1A6A1A06046728).

References

1. J. C. Love, L. A. Estroff, J. K. Kriebel, R. G. Nuzzo, G. M. Whitesides, *Chem. Rev.* **2005**, *105*, 1103.
2. M. Kind, C. Wöll, *C. Prog. Surf. Sci.* **2009**, *84*, 230.
3. S. Casalini, C. A. Bortorotti, F. Leonardi, F. Biscarini, *Chem. Soc. Rev.* **2017**, *46*, 40.
4. M. Waldrip, O. D. Jurchescu, D. J. Gundlach, E. G. Bittle, *Adv. Funct. Mater.* **2020**, *30*, 1904576.
5. J. Chen, S. Gathiaka, Z. Wang, M. Thuo, *J. Phys. Chem. C* **2017**, *121*, 23931.
6. B. Lee, S. Takeda, K. Nakajima, J. Noh, J. Choi, M. Hara, T. Nagamune, *Biosens. Bioelectron.* **2004**, *19*, 1169.
7. S. Han, S. Seong, Y. J. Son, Y. Yokota, T. Hayashi, M. Hara, *J. Phys. Chem. C* **2020**, *124*, 26730.
8. T. Park, H. Kang, S. Seong, S. Han, Y. J. Son, E. Ito, T. Hayashi, M. Hara, J. Noh, *J. Phys. Chem. C* **2019**, *123*, 9096.
9. A. Tsunoi, G. Lkhamsuren, E. A. Q. Mondarte, S. Asatyas, M. Oguchi, J. Noh, T. Hayashi, *J. Phys. Chem. C* **2019**, *123*, 13681.
10. S. Y. Lee, E. Ito, H. Kang, M. Hara, H. Lee, J. Noh, *J. Phys. Chem. C* **2014**, *118*, 8322.
11. H. Lu, M. Kind, A. Terfort, M. Zharnikov, *J. Phys. Chem. C* **2013**, *117*, 26166.
12. E. Ito, J. Noh, M. Hara, *Jpn. J. Appl. Phys.* **2003**, *42*, L852.
13. D. Lee, S. Seong, J. Noh, *Bull. Kor. Chem. Soc.* **2019**, *40*, 619.

14. H. Kang, S. Seong, S. Han, Y. J. Son, J. Park, J. Noh, *Bull. Kor. Chem. Soc.* **2019**, *40*, 299.
15. H. Kang, E. Ito, M. Hara, J. Noh, *J. Nanosci. Nanotechnol.* **2016**, *16*, 2800.
16. W. Azzam, A. Subaihi, *Surf. Interfaces* **2020**, *20*, 100544.
17. S. Seong, H. Kang, S. Han, T. Sung, J. B. Park, T. Hayashi, M. Hara, J. Noh, *J. Nanosci. Nanotechnol.* **2017**, *17*, 5597.
18. M.-S. Han, K. Ku, H. Kang, R. Ohashi, T. Hayashi, M. Hara, J. Noh, *J. Nanosci. Nanotechnol.* **2017**, *17*, 5780.
19. E. Ito, H. Kang, D. Lee, J. B. Park, M. Hara, J. Noh, *J. Colloid, Interf. Sci.* **2013**, *394*, 522.
20. L. T. M. Huynh, S. Lee, S. Yoon, *Bull. Kor. Chem. Soc.* **2019**, *40*, 839.
21. M. Hong, Y. Yokota, N. Hayazawa, E. Kazuma, Y. Kim, *J. Phys. Chem. C* **2020**, *124*, 13141.
22. Ö. Kap, N. Kabanov, M. Tsvetanova, C. Varlikli, A. L. Klacsyk, H. J. W. Zandvliet, K. Sottewes, *J. Phys. Chem. C* **2020**, *124*, 11977.
23. J. Noh, K. Kobayashi, H. Lee, M. Hara, *Chem. Lett.* **2000**, *29*, 630.
24. J. Noh, M. Hara, *Langmuir* **2002**, *18*, 9111.
25. N.-S. Lee, D. Kim, H. Kang, D. K. Park, S. W. Han, J. Noh, *J. Phys. Chem. C* **2011**, *115*, 5868.
26. D. A. Krachetov, H. Ma, A. K. Y. Jen, D. A. Fischer, Y.-L. Loo, *Langmuir* **2008**, *24*, 851.
27. L. Cai, Y. Yao, J. Yang, D. W. Price, J. M. Tour, *Chem. Mater.* **2002**, *14*, 2905.
28. B. T. Holmes, A. W. Snow, *Tetrahedron* **2005**, *61*, 12339.
29. M. I. Béthencourt, L. Srisombat, P. Chinwangso, T. R. Lee, *Langmuir* **2009**, *25*, 1265.
30. J. W. Ciszek, M. P. Stewart, J. M. Tour, *J. Am. Chem. Soc.* **2004**, *126*, 13172.
31. Y. Choi, Y. Jeong, H. Chung, E. Ito, M. Hara, J. Noh, *Langmuir* **2008**, *24*, 91.
32. S. Y. Lee, Y. Choi, E. Ito, M. Hara, H. Lee, J. Noh, *Phys. Chem. Chem. Phys.* **2013**, *15*, 3609.
33. Y. Choi, S. Seong, Y. J. Son, S. Han, E. Ito, E. A. Q. Mondarte, R. Chang, T. Hayashi, M. Hara, J. Noh, *Colloid Surf. A-Physicochem. Eng. Asp.* **2019**, *583*, 123969.
34. R. I. Giinther, M. C. Lee, A. F. Raigoza, *Surf. Sci.* **2020**, *694*, 121562.
35. Y. Choi, S. Seong, S. Han, Y. J. Son, E. A. Q. Mondarte, H. Tahara, S. Song, T. Hayashi, J. Noh, *Thin Solid Films* **2020**, *707*, 138100.
36. Z. Ng, K. P. Loh, L. Li, P. Ho, P. Bai, J. H. K. Yip, *ACS Nano* **2009**, *3*, 2103.
37. A. S. Blum, J. C. Yang, R. Shashidhar, B. Ratna, *Appl. Phys. Lett.* **2003**, *82*, 3322.
38. H. Valkenier, E. H. Huisman, P. A. van Hal, D. M. de Leeuw, R. C. Chiechi, J. C. Hummelen, *J. Am. Chem. Soc.* **2011**, *133*, 4930.
39. Q. Zhou, A. Yamada, Q. Feng, A. Hoskins, B. D. Dunietz, K. M. Lewis, *ACS Appl. Mater. Interfaces* **2017**, *9*, 15901.
40. A. Yamada, Q. Feng, Q. Zhou, A. Hoskins, K. M. Lewis, *J. Phys. Chem. C* **2017**, *121*, 10298.
41. J. M. Tour, L. Jones, D. L. Pearson, J. J. S. Lamba, T. P. Burgin, G. M. Whitesides, D. L. Allara, A. N. Parikh, S. V. Atre, *J. Am. Chem. C* **1995**, *117*, 9529.
42. Y. Kang, D. Won, S. Kim, K. Seo, H. Choi, G. Lee, Z. Noh, T. Lee, C. Lee, *Mater. Sci. Eng. C* **2004**, *24*, 43.
43. Y. Jeong, S. Kwon, Y. Kang, C. Lee, E. Ito, M. Hara, J. Noh, *Ultramicroscopy* **2007**, *107*, 1000.
44. Y. Jeong, C. Lee, E. Ito, M. Hara, J. Noh, *Jpn. J. Appl. Phys.* **2006**, *45*, 5906.
45. T. Park, H. Kang, Y. Kim, S. Lee, J. Noh, *Bull. Kor. Chem. Soc.* **2011**, *32*, 39.
46. T. Park, H. Kang, I. Choi, H. Chung, E. Ito, M. Hara, J. Noh, *Bull. Kor. Chem. Soc.* **2009**, *30*, 441.
47. A. Bashir, D. Iqbal, S. M. Jain, K. Barbe, T. Abu-Husein, M. Rohwerder, A. Terfort, M. Zharnikov, *J. Phys. Chem. C* **2015**, *119*, 25352.
48. A. Singh, D. H. Dahanayaka, A. Biswas, L. A. Bumn, R. L. Halterman, *Langmuir* **2010**, *26*, 13221.
49. J. J. Stapleton, P. Harder, T. A. Daniel, M. D. Reinard, Y. Yao, D. W. Price, J. M. Tour, D. L. Allara, *Langmuir* **2003**, *19*, 8245.
50. A. Shaporenko, M. Elbing, A. Blaszczyk, C. von Hänisch, M. Mayor, M. Zharnikov, *J. Phys. Chem. B* **2006**, *110*, 4307.
51. J. L. Donhauser, B. A. Mantooth, K. F. Kelly, L. A. Bumn, J. D. Monnell, J. J. Stapleton, D. W. Price, A. M. Rawlett, D. L. Allara, J. M. Tour, P. S. Weiss, *Science* **2001**, *292*, 2303.
52. L. Cheng, J. Yang, Y. Yao, D. W. Price, M. D. Shawn, J. M. Tour, *Langmuir* **2004**, *20*, 1335.
53. R. Yamada, H. Sakai, K. Uosaki, *Chem. Lett.* **1999**, *28*, 667.
54. N.-S. Lee, H. Kang, E. Ito, M. Hara, J. Noh, *Bull. Kor. Chem. Soc.* **2010**, *31*, 2137.
55. A. H. A. Mamun, J. R. Hahn, *J. Phys. Chem. C* **2012**, *116*, 22441.
56. J. Dai, Z. Li, J. Jin, J. Cheng, J. Kong, S. Bi, *J. Electroanal. Chem.* **2008**, *624*, 315.
57. S. Y. Lee, J. Noh, E. Ito, H. Lee, M. Hara, *Jpn. J. Appl. Phys.* **2003**, *42*, 236.
58. C.-W. Fu, T.-H. Lin, *J. Phys. Chem. A* **2011**, *115*, 13523.
59. N.-S. Lee, H. Kang, S. Seong, J. Noh, *Bull. Kor. Chem. Soc.* **2019**, *40*, 1152.
60. J. Noh, M. Hara, *Langmuir* **2002**, *18*, 1953.
61. A. H. A. Mamun, J. R. Hahn, *Surf. Sci.* **2012**, *606*, 664.
62. F. Li, L. Tang, W. Zhou, Q. Guo, *J. Am. Chem. Soc.* **2010**, *132*, 13059.
63. D. G. Castner, K. Hinds, D. W. Grainger, *Langmuir* **1996**, *12*, 5083.
64. T. Ishida, M. Hara, I. Kojima, S. Tsuneda, N. Nishida, H. Sasabe, W. Knoll, *Langmuir* **1998**, *14*, 2092.
65. T. Ishida, N. Choi, W. Mizutani, H. Tokumoto, I. Kojima, H. Azebara, H. Hokari, U. Akiba, M. Fujihira, *Langmuir* **1999**, *15*, 6799.
66. F. Chesneau, J. L. Zhao, C. Shen, M. Buck, M. Zharnikov, *J. Phys. Chem. C* **2010**, *114*, 7112.